Spotlight on Molecular Profiling

Predicting cisplatin and trabectedin drug sensitivity in ovarian and colon cancers

Ellen V. Stevens,[1] Satoshi Nishizuka,[1] Smitha Antony,[1] Mark Reimers,[1] Sudhir Varma,[1] Lynn Young,[3] Peter J. Munson,[3] John N. Weinstein,[1] Elise C. Kohn,[2] and Yves Pommier[1]

[1]Laboratory of Molecular Pharmacology and [2]Laboratory of Pathology, Center for Cancer Research and [3]Mathematical and Statistical Computing Laboratory, Center for Information Technology, National Cancer Institute, NIH, Bethesda, Maryland

Abstract

Molecular profiling of markers involved in the activity of chemotherapeutic agents can shed light on the successes and failures of treatment in patients and can also provide a basis for individualization of therapy. Toward those ends, we have used reverse-phase protein lysate microarrays to evaluate expression of protein components of the nucleotide excision repair (NER) pathways. Those pathways strongly influence the anticancer activities of numerous drugs, including those that are the focus here, cisplatin and ecteinascidin 743 (Et-743; Yondelis, Trabectedin). Cisplatin is generally more active in cell types deficient in NER, whereas Et-743 tends to be less active in those cells. We measured protein expression and sensitivity to those drugs in 17 human ovarian and colon cancer cell lines (13 of them from the NCI-60 panel) and five xeroderma pigmentosum (XP) patient cell types, each containing a different NER defect. Of the NER proteins giving reliable signals, XPF and XPG showed the highest correlations of protein expression with drug activity across all three tissue-of-origin groups. When we compared protein expression data with mRNA expression data from Affymetrix U133A chips, we found no consistent correlation between the two across the cell lines studied, which reinforces the conclusion that protein measurements can give more interpretable mechanistic information than can transcript measurements. The work reported here provides motivation for larger proteomic studies with more cell types focused on potential biomarkers in additional pharmacologically pertinent pathways. [Mol Cancer Ther 2008;7(1):10–8]

Introduction

Platinum derivatives are the mainstay of chemotherapy for many epithelial malignancies, including ovarian and colon cancers (1). For many advanced cancers, the rate of response to initial chemotherapy is quite high, but the patients tend to relapse (and then to be more refractory to second or third line treatment; ref. 2). For instance, 70% to 80% of advanced stage ovarian cancers respond to cisplatin-based primary therapy, with around 50% of the responders eventually relapsing due to clinical resistance (2). Nucleotide excision repair (NER) is the primary mechanism known to remove platinum-DNA adducts (including cisplatin-induced and oxaliplatin-induced intrastrand crosslinks) from DNA (1, 3–5), thereby increasing resistance to the drug. NER is composed of two subpathways for damage detection: (*a*) global genome NER, which maintains the integrity of the entire genome, and (*b*) transcription-coupled NER (TC-NER), which accounts for removal of damage in the transcribed strands of active genes. Impaired NER activity is associated with several rare autosomal recessive photosensitivity diseases, including xeroderma pigmentosum (XP), Cockayne syndrome, and trichothiodystrophy (6). NER factors are also mutated in some human cancers, including ovarian and testicular tumors (3, 7, 8), and can therefore contribute to clinical resistance to platinum derivatives (1).

Global genome NER and TC-NER are comparable in terms of mechanism, except for the initial damage recognition step (6). In global genome NER, helix-distorting base lesions are identified by XPC-hHR23B. In TC-NER, elongating RNA polymerase II encounters the lesion and recruits the Cockayne syndrome factors CSA and CSB. Subsequent stages of the two subpathways are the same. TFIIH is composed of XPB and XPD, helicase components that catalyze ATP-dependent unwinding of the DNA strands. XPA and replication protein A stabilize the open complex and position the other factors. Dual incision is done by ERCC1-XPF and XPG endonucleases, which cleave the damaged strand 5′ to 3′ of the lesion, respectively.

Received 3/19/07; revised 9/28/07; accepted 12/4/07.

Grant support: Intramural Research Program of the Center for Cancer Research, National Cancer Institute, NIH.

The costs of publication of this article were defrayed in part by the payment of page charges. This article must therefore be hereby marked *advertisement* in accordance with 18 U.S.C. Section 1734 solely to indicate this fact.

Note: E.C. Kohn and Y. Pommier contributed equally to this manuscript.

Requests for reprints: Yves Pommier, National Cancer Institute, Building 37, Room 5068, Bethesda, MD 20892. Phone: 301-496-5944; Fax: 301-402-0752. E-mail: pommier@nih.gov

doi:10.1158/1535-7163.MCT-07-0192

Finally, NER is completed by gap-filling DNA synthesis, followed by strand ligation.

Ecteinascidin 743 (Et-743; Yondelis, Trabectedin), a natural product isolated from a marine tunicate, is currently under registration for the treatment of soft tissue sarcomas and is being studied in a pivotal Phase III trial for ovarian cancer[4] (9, 10). The mechanism by which Et-743 interacts with DNA and exerts its antitumor activity is different from those of other alkylating agents, such as cisplatin. Whereas cisplatin binds to the N7 position of guanine in the major groove of DNA (1), Et-743 forms monoadducts at the N2 position of guanine in the minor groove of DNA, forcing the minor groove toward the major groove and allowing possible interaction of the C-ring portion of the drug with the NER factors (11, 12). Although the precise mechanism of action of Et-743 has not been fully elucidated, Et-743 has been found to be more active in cells with an enhanced TC-NER system, for example, in cisplatin-resistant cells (4, 13, 14). An understanding of the opposite relationships of cisplatin and Et-743 with the NER pathways could be useful, potentially yielding more effective molecularly targeted treatment strategies and suggesting that Et-743 could be used in a second-line regimen after cisplatin-based treatment or in combination with cisplatin.

To further our understanding of the relationship between NER and resistance to cisplatin and Et-743, we studied the expression of NER factors and the sensitivity to those two drugs in a set of cell types that express different levels of the NER components. Generally, that approach would involve assessment of transcript levels, for example, using oligonucleotide microarrays. However, it is well understood that transcript levels may or may not accurately reflect protein levels, depending on the particular molecular species and the biological specimens to be compared; see, for example, refs. (15, 16). Because proteins are the directly acting molecules in the NER pathway and the species most often useful as clinical biomarkers, we preferred to profile the proteins rather than the transcripts. In the present study, therefore, we used a high-throughput proteomic technology, the reverse-phase protein lysate microarray, to quantitate NER components and other proteins in ovarian cancer, colon cancer, and XP patient cells. One advantage of the reverse-phase microarray technology (15, 17) is that it permits direct comparison for a given protein species across samples on a single glass slide. That type of comparison is more useful than a direct comparison of different proteins in a given sample, as is obtained from two-dimensional gels, antibody arrays, and most mass spectrometry–based technologies.

After obtaining the NER protein profiles across cell lines, we compared them with patterns of sensitivity to Et-743 and cisplatin, which we determined using the 3-(4,5-dimethylthiazol-2-yl)-2,5-diphenyltetrazolium bromide (MTT) assay. XPF and XPG showed the highest correlation with drug activity in the set of cell lines studied. Thirteen of the 17 colon and ovarian cancer cell types are included in the panel of 60 human cancer cell lines (NCI-60) used by the National Cancer Institute (NCI) to screen for anticancer agents (18). It will, therefore, be possible in future analyses to relate the NER protein expression levels presented here to the overall database of compounds screened and also to the large array of additional molecular characterizations of the NCI-60 at the DNA, RNA, protein, and small molecule levels. Those characterizations are represented in the ''Spotlight on Molecular Profiling'' series, inaugurated by Molecular Cancer Therapeutics in November of 2006 (19).

Materials and Methods

Cells, Drugs, and Antibodies

OVCAR3, OVCAR4, OVCAR5, OVCAR8, Igrov1, and Skov3 ovarian cancer cells were provided by Dr. R. Camalier, Division of Cancer Treatment and Diagnosis Tumor Repository, NCI. A2780 ovarian cancer cells and the cisplatin-resistant variant CP70 were provided by Dr. T. Fojo (Cancer Therapeutics Branch, NCI). The HeyA8 ovarian cancer cell line was provided by Dr. G. Mills of M.D. Anderson Cancer Center. HCC2998, SW620, HT29, COLO205, HCT15, KM12, and HCT116 colon cancer cells were purchased from the American Type Culture Collection. The Et-743–resistant HCT116 variant HCT116/ER5 has been reported previously (13). GM637 normal nonfetal transformed fibroblasts, GM4312 (XPA) transformed fibroblasts, GM2345 (XPB) transformed lymphoblasts, GM8207 (XPD) transformed fibroblasts, and GM8437 (XPF) transformed fibroblasts cells were purchased from Human Genetic Mutant Cell Repository, Coriell Institute for Medical Research. The XP20BE (XPG) primary fibroblast cell line was provided by Dr. K. Kraemer (Laboratory of Molecular Carcinogenesis, NCI). Cells lines were maintained in RPMI or DMEM supplemented with 10% fetal bovine serum. All cell lines were regularly tested for *Mycoplasma* contamination by PCR analysis.

Et-743 was provided by the NCI Developmental Therapeutics Program, NCI. Cisplatin was purchased from Sigma. Anti-XPA, anti-ERCC1, anti-DNA polymerase β, anti-Rad51, anti–X-ray complementing defective 1 gene, anti–mismatch repair protein 2 (MSH2), anti-p300, anti–keratin 8, anti–keratin 7, anti–proliferating cell nuclear antigen, anti-MSH6, and anti–Ref 1 monoclonal antibodies were purchased from Neomarkers. Anti-XPB rabbit polyclonal antibody was obtained from Santa Cruz Biotechnology. Anti–breast cancer 1 gene monoclonal antibody (21A8) was donated by Dr. T. Ouchi from New York University. Anti-XPD was donated by Dr. J. Bradsher from NCI. Anti-XPC, anti-XPF, and anti-XPG rabbit polyclonal antibodies were donated by Dr. R. Wood of University of Pittsburgh. Secondary alkaline phosphatase–conjugated goat anti-rabbit and goat anti-mouse antibodies were purchased from Tropix.

[4] http://www.pharmamar.com/en/pipeline/yondelis.cfm

Protein Lysate Preparation and Micro–Western Blot Analysis

Cell lines were grown to 50% to 80% confluence, then scraped from the flask and washed thrice with cold PBS. Cell pellets were lysed in buffer as described previously (15). Lysates were aliquoted and stored at −80°C to avoid repeated freeze/thaw cycles, and antibody specificity was determined by micro–Western blotting. Samples containing 10 μg of protein in an SDS standard loading buffer were electrophoresed in a 4% to 20% Tris-glycine Novex precise gels. After electrophoresis, the separated proteins were transferred to a nitrocellulose membrane, which was then incubated with I-Block blocking buffer (Tropix) with 0.1% Tween 20. The blot was incubated with specific primary antibodies and then incubated with secondary alkaline phosphatase–conjugated antibody. Protein bands were visualized by chemiluminescence using CDP-Star ready-to-use substrate solution (Tropix).

Reverse-Phase Protein Lysate Arrays

Arrays were designed and produced as previously described (15). Briefly, lysate samples were manually loaded into 384-well microtiter plates (Genetix) to produce ten 2-fold serial dilutions at a constant buffer composition for each sample. Arrays were made in batches of 20 by spotting samples from the microtiter plates onto 20 nitrocellulose-coated glass slides (FAST Slides, Schleicher & Schuell) using a pin-in-ring format Affymetrix GMS 417 arrayer. Lysate samples in microtiter plates were freeze/thawed no more than thrice. Arrays were stored at −20°C until use. The 1st and 20th array of each batch were stained for total protein using Sypro ruby protein blot stain (Molecular Probes) and scanned using a FluorImager SI (Amersham Pharmacia Biotech) at 100-μm resolution. The 2nd and 19th slides were stained with anti-p300 antibody to provide interbatch and intrabatch controls, and the remaining slides were stained with antibodies of interest. Slides 2 to 19 were processed through an automated Autostainer using the catalyzed signal amplification staining system (DAKO). Slides were then scanned with an ordinary optical flatbed scanner, the Perfection 1200S (Epson America), and the array spot images were converted to raw pixel values using the Peak Quantification with Statistical Comparative Analysis program.[5]

The dose interpolation algorithm (DI_{25}), developed in a previous study (15), was used to analyze the array data. Briefly, the 25th percentile of each dose-response curve for each cell line was calculated for both target and total protein levels. Each experimental DI_{25} value was adjusted by total protein level for each cell line. Throughout this article, the term ''protein level'' from the microarrays refers to the DI_{25} value, which is expressed in terms of the 2-fold dilution number, hence in terms of a relative log base 2 of the protein expression level. Clustered image maps (20), also known as clustered ''heat maps,'' were generated using the CIMMiner program.[6] The clustered image maps represent data from the 26 antibodies tested against the 24 cell lines, including two replicates of GM637 (normal nonfetal transformed fibroblast) cells.

Growth Inhibition Assay

The MTT assay was done to determine the relative sensitivities of cell lines to cisplatin and Et-743. Cells were seeded in six replicates at 1,000 to 5,000 cells per well in 96-well plates, incubated overnight, and exposed to serial dilutions of cisplatin or Et-743 continuously for 72 h. The drug-containing medium was removed and replaced by medium containing MTT (Sigma), after which the cells were incubated for 4 h at 37°C. After removal of the MTT, DMSO was added, and the absorbance was measured at 560 nm using a microplate reader. The results were expressed relative to the absorbance of cells grown in the absence of drug. IC_{50} values were calculated by nonlinear regression analysis from triplicate independent experiments using GraphPad Prism software.

Results

Protein Expression Profile of the NER Pathway in Ovarian Cancer Cell Lines

NER protein levels in ovarian cell lines and cell lines derived from XP patients (XPA, XPB, XPD, XPF, and XPG) are shown in Fig. 1. Included were six ovarian lines from the NCI-60 screen. Strong expression of XPD was observed in all of the cells, whereas other NER proteins were expressed to various extents in the different cell lines. For instance, many of the NER proteins were more strongly expressed in OVCAR3 and OVCAR5 than in OVCAR4, which expressed lower levels of XPA and XPF. The large differences in NER protein levels within the ovarian cancer cell line panel suggest possible functional differences in the pathway.

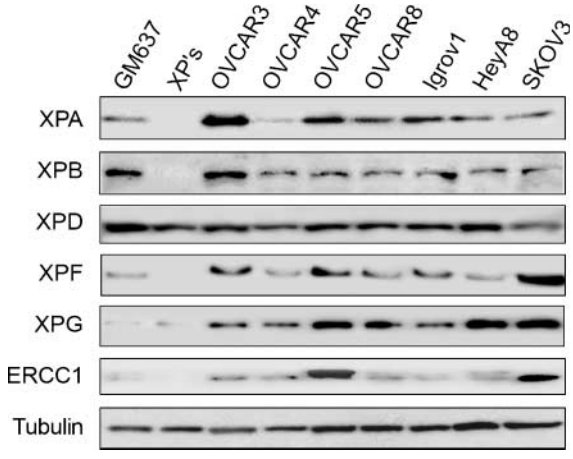

Figure 1. XP protein expression levels. Micro–Western blots of extracts from ovarian cancer and XP patient (XPA, XPB, XPD, XPF, and XPG) cell lines (*top*) probed with antibodies against NER proteins. For ERCC1, the XPF patient cell line was used because there is no ERCC1 patient cell line. GM637 are normal nontransformed human fetal fibroblasts. Tubulin was used as a loading control.

[5] Available at http://abs.cit.nih.gov/pscan.
[6] Available at http://discover.nci.nih.gov.

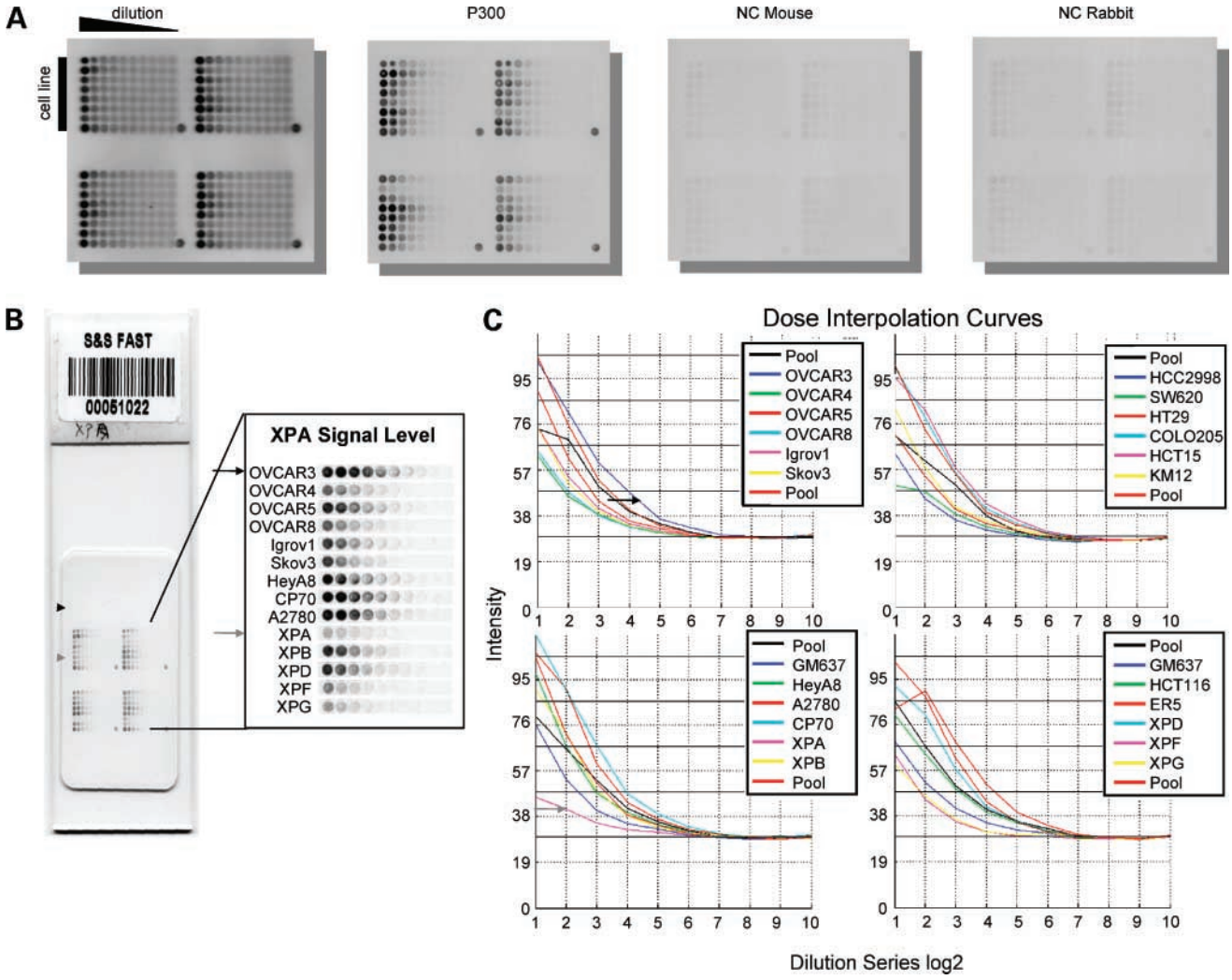

Figure 2. Reverse-phase protein lysate microarray. **A,** control slides include total protein staining with Sypro Ruby, CSA staining with p300, and negative controls (*NC*) with irrelevant mouse and rabbit IgGs (anti–*Aspergillus niger*) in place of the p300-specific antibody. **B,** CSA staining with XPA. **C,** dilution-intensity curves for each cell line on the array. *Y* axes, Peak Quantification with Statistical Comparative Analysis intensity read-outs; *X* axes, 2-fold dilution series.

Validation of Reverse-Phase Protein Lysate Microarrays in Application to NER

Differences in the NER pathway among ovarian and colon tumor cell lines were quantitated by using reverse-phase protein lysate microarrays. On Western blot, each antibody selected for the reverse microarray studies gave a specific and prominent band whose electrophoretic migration corresponded to the expected molecular mass of the target protein. Each array included ten 2-fold serial dilutions of each cell line and eight control lysate pools (prepared by mixing equal volumes of all of the cell lines together). Similar amounts of total protein were loaded on the array for all of the cell lines. Mouse and rabbit anti–*Aspergillus niger* glucose oxidase IgG1, used as a negative control antibody, showed only low, nonspecific signals (Fig. 2A). The median Pearson's correlation coefficient was +0.95 for the six pairwise comparisons of four replicate p300 arrays across all of the cell lines on the arrays. The dilution curves for XPA protein expression (Fig. 2B) are shown in Fig. 2C. OVCAR3 expressed the highest levels of XPA. The Spearman's (nonparametric) correlation coefficient between the micro–Western blot probing for XPA and the lysate microarray DI_{25} value was +0.84. Collectively, the results indicate that data from the arrays developed for this study of NER proteins are reproducible and quite reasonably concordant with the data from micro–Western blots.

Next, we tested the relationship between protein expression and mRNA levels. The mRNA levels were derived from our prior profiling of the NCI-60 using Affymetrix HG-U133 chips (16). None of the NER factors tested (XPA, XPC, XPF, and XPG) gave a significant correlation between mRNA and protein expression (all of the Pearson correlation coefficients were below 0.21). Rad51 gave a correlation

coefficient of 0.27. Only p300 showed a significant correlation between mRNA and protein (Pearson correlation coefficient, 0.63; $P < 0.02$). Together those results suggest that proteins of the NER pathways should be measured directly rather than depending on the mRNA as a surrogate.

In addition, we compared the NER protein profiles with compound sensitivity [$-\log_{10}(GI_{50})$] in the ovarian and colon cancer cell lines from the NCI-60 cell database (16, 21) and found a negative correlation between sensitivity to nitrosoureas and XPA protein levels (Table 1). The Pearson correlation coefficients were −0.77 for lomustine [1-(2-chloroethyl)-3-cyclohexyl-L-nitrosourea] and −0.60 for carmustine [1,3-bis(2-chloroethyl)-1-nitrosourea], whereas nonalkylating agents showed no correlation (correlation of −0.26 for doxorubicin, −0.03 for L-asparaginase, 0.02 for hydroxyurea, and 0.25 for paclitaxel).

Clustered Image Map Representation of the Expression Profiles of NER and Other Proteins

Many other factors, including repair pathways, may be involved in the cisplatin resistance of cancer cells. We therefore assessed the protein expression of a number of molecules that might show related changes: p53 (tumor suppressor protein p53), MSH2, p300 (E1A-binding protein), Rad51 (RecA homologue), keratin 8, keratin 7, proliferating cell nuclear antigen, poly[ADP-ribose] polymerase, DNA polymerase β, X-linked inhibitor of apoptosis, nuclear factor-κB, MSH6, X-ray complementing defective 1 gene, breast cancer 1 gene, and Ref1 (multifunctional DNA repair enzyme). Clustered image map–relating cells and proteins were generated using the calculated DI_{25} values (Fig. 3). All replicate samples clustered side by side with high positive Pearson's correlation coefficients. For example, the GM637 cell line replicates clustered together with a correlation coefficient of +0.89, and the mean correlation coefficient for XPA, XPC, XPF, and XPG duplicate arrays was +0.92. Overall, the ovarian cancer and colon cancer cell lines did not cluster well by tissue-of-origin groups. A2780 and the A2780 cisplatin–resistant derivative CP70 clustered tightly with a Pearson correlation of +0.98. HCT116 and its Et-743 resistant derivative, ER5 (13), did not cluster tightly. HCT116 expressed higher levels of keratin 8, Rad51, and Ref1, whereas ER5 expressed higher levels of MSH2, p53, X-linked inhibitor of apoptosis, and nuclear factor-κB. ER5, with a mutation in the XPG gene, expressed lower protein levels of XPG, XPF, and XPC (13). HCT116 is deficient in MSH2, and the array indeed showed low expression of that protein (22). Similarly, HCT15, known to be deficient in MSH6, expressed low amounts of that protein (23). Keratin 8, expressed in epithelial cancers, was expressed strongly in the colon and ovarian cancers with the exception of ER5, A2780, CP70, Igrov1, HeyA8, OVCAR5, and Skov3 (24). In contrast, keratin 7, an ovarian cancer marker, was expressed most prominently in the ovarian cell lines except for Igrov1, A2780, and CP70 (25). Igrov1 was the only ovarian line that did not express MSH2. The XPB and XPD cell lines clustered tightly, an interesting observation because both XPB and XPD function as helicases in the TFIIH NER complex to unwind DNA at the damage site. Cell lines from XP patients are known to express higher levels of p53 (26). The XPA, XPB, XPD, and XPF cell lines did, in fact, express high levels of p53. However, XPG, the only XP patient line we studied that is a nontransformed primary cell line, did not. Overall, the clustered image map showed the protein expression measurements to be technically reliable and biologically reasonable.

Table 1. Correlation between XPA protein expression and drug activity in the ovarian and colon cell lines from the NCI-60 cell screen

NSC number	Drug name	XPA versus $\log_{10}(GI_{50})$
79037	Lomustine (CCNU)	−0.77
409962	Carmustine (BCNU)	−0.60
353451	Mitozolamide	−0.66
122819	Teniposide	−0.03
109229	L-Asparaginase	−0.03
32065	Hydroxyurea	0.03
752	Thioguanine	0.26
125973	Taxol (Paclitaxel)	0.26

NOTE: Pearson correlation was calculated between the negative $\log_{10}(GI_{50})$ and XPA protein expression (21).
Abbreviations: CCNU, 1-(2-chloroethyl)-3-cyclohexyl-L-nitrosourea; BCNU, 1,3-bis(2-chloroethyl)-1-nitrosourea.

Cisplatin and Et-743 Have Different Activity Profiles

In the MTT assay, Et-743 and cisplatin showed different profiles of activity across the ovarian cancer, colon cancer, and XP patient cell lines (Fig. 4). The NER-deficient patient cell lines (XPA, XPB, XPD, XPF, and XPG) were, as a group, more sensitive to cisplatin than to Et-743. In comparison with GM637, the XP-deficient lines were more Et-743 resistant and cisplatin sensitive. Among the colon lines tested, HCC2998 and HT29 were highly resistant to cisplatin and sensitive to Et-743. In contrast, HCT15 and ER5 were highly resistant to Et-743 and sensitive to cisplatin. The ovarian lines OVCAR4 and Skov3 were sensitive to cisplatin and somewhat resistant to Et-743. The opposite was true for CP70, HeyA8, and OVCAR8, which were more sensitive to Et-743 and resistant to cisplatin. In the other ovarian and colon lines, the two drugs were similar in their potency.

Best NER Predictors of Et-743 and Cisplatin Drug Sensitivity

Developing more effective molecularly targeted therapies requires identification of biomarkers that predict sensitivity and resistance. In the present study, we attempted to identify potential biomarker proteins by assessing correlations between their expression levels and relative sensitivities to cisplatin and Et-743. To obtain a ''drug preference score,'' we subtracted the sensitivity (expressed as minus the logarithm base 10 of the 50% growth inhibitory concentration) to Et-743 from that to cisplatin. We then computed the correlation coefficient between that preference score and the expression level of each of the proteins profiled, focusing on the XP family (Table 2). Many of the

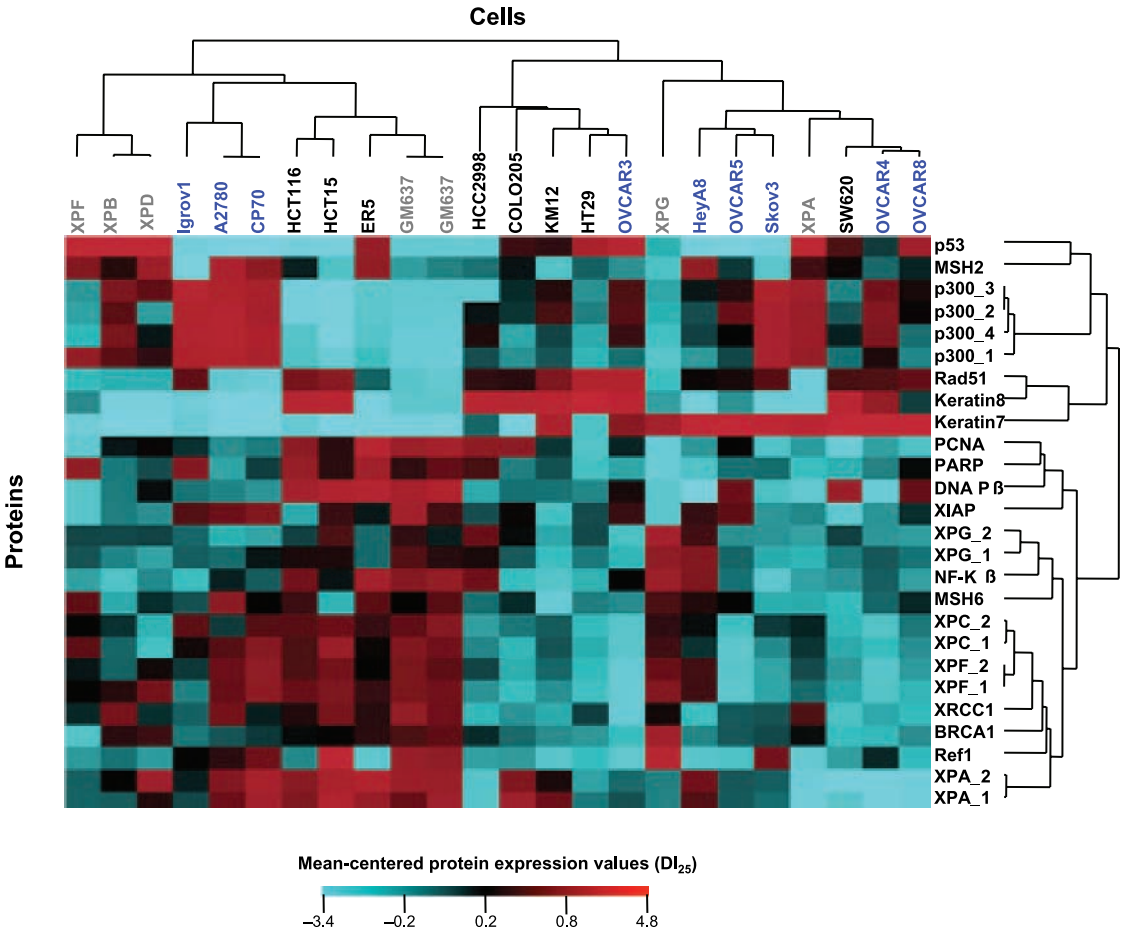

Figure 3. Clustered image map relating protein expression levels and cell lines; *blue,* ovarian lines; *black,* colon lines; *gray,* XP patient and fibroblasts lines. Average linkage clustering with Pearson's correlation coefficient similarity measure was used to produce the map. The height on the dendrogram is defined as $1 - r$, wherein r is the Pearson correlation coefficient. DI_{25} values were mean-centered across both cells and proteins, so the mean correlation is ~0.

proteins showed moderate correlations with the drug preference score, but the correlations were not highly significant. For instance, within the XP cell lines group, the P value equaled 0.09, as computed by randomly permuting the cell lines labels for proteins and recomputing the correlations.

We also investigated correlations within tissue-of-origin groups and found several cases in which protein levels seemed to predict relative activities of cisplatin and Et-743. For example, levels of Rad51 showed a correlation of 0.55 with ''cisplatin preference'' among the ovarian lines, but an opposite correlation of −0.78 with cisplatin among the colon lines. Several other proteins showed similar patterns. Such large positive and negative correlations would quite possibly achieve statistical significance in a study based on a larger sample set, but they were only marginally significant (P = 0.07 by randomization test) for the small samples studied here. That is, they generated hypotheses to be investigated further.

Of the NER proteins, XPF and XPG showed the highest correlations with drug activity across all three tissue-of-origin groups (ovarian cancer, colon cancer, and XP cell lines). The increased protein expression was directly correlated with Et-743 sensitivity and cisplatin resistance. Those proteins were especially effective in predicting cisplatin and Et-743 activity in the NER-deficient lines but were only moderately well correlated with drug activity for the ovarian and colon tissue-of-origin groups (multiple comparisons–corrected P values were P = 0.11 for XPG and P = 0.16 for XPF in randomization tests for ovarian and colon lines taken together). The differences observed in the panel of cell lines in the present study are consistent with the differential sensitivity to Et-743 and cisplatin of isogenic cell lines differentially expressing NER factors (4, 13).

Discussion

Promising evidence of antitumor activity and clinical benefit have been reported for Et-743 in clinical trials for many cancer types, including soft tissue sarcomas, breast cancers, and ovarian cancers (10, 27– 30). A phase II clinical trial of Et-743 showed promising activity in relapsed ovarian cancer patients (31). As with other therapeutic

agents, one is prompted to ask whether the success rate could be increased if therapy was selected on the basis of molecular profiles of the tumors. In the case of Et-743, logical molecules to consider as candidate biomarkers are the NER components. Et-743, in contrast, for example, to cisplatin (which is also used clinically against ovarian cancer), has been reported to be more active against NER intact cells than against NER-deficient ones. Although the role of NER in relation to the clinical activity of Et-743 and cisplatin remains to be understood comprehensively, the TC-NER pathway has been implicated in sensitivity and resistance of tumor cell lines to those drugs. Cells deficient in TC-NER have been reported as hypersensitive to UV radiation, cisplatin, and other alkylating agents, but resistant to Et-743 (4, 13, 14, 32). However, contradictory results have been published from various investigators attempting to correlate resistance to cisplatin therapy with elevated levels of genes and proteins of the NER pathway (1, 3, 33–37).

Here, we report expression profiles of the NER molecules in cells from five XP patients with various known NER defects and in a set of ovarian and colon cancer cell lines (all but four of them from the NCI-60 panel). Because of the opposite influences of NER defects on the activity of Et-743 and cisplatin (4, 13), we then asked how the expression levels relate to differences in activity between the two drugs. The simplest approach to profiling would have been at the transcript level, for example, by oligonucleotide microarray or reverse transcription–PCR. However, the relationship between transcript and protein expression is unknown for NER molecules, and the proteins are the directly active molecules. Hence, we used the reverse-phase lysate microarray platform for quantitation at the protein level (15, 17). That technology served our present purpose well, because it permitted direct comparison for each protein across all of the cell types on a single glass slide. To validate the microarray platform, we compared its results with those from micro–Western blots; the concordance was strong (e.g., +0.84 Spearman correlation for XPA). We also found the arrays to be highly reproducible (+0.95 correlation for replicate arrays assessing the control protein p300). We previously reported that some gene families show good correlation across the NCI-60 between transcript and protein expression profiles and some do not. In this study, the transcript and protein levels of NER molecules were poorly correlated. In general, proteomic profiling may yield more direct answers than transcript profiling because the majority of known biological effector molecules, diagnostic markers, and pharmaceutical targets are proteins (38, 39). It may be possible to hit pharmacologic targets more selectively if the pertinent pathways and their regulation are better understood at the protein level.

Individually, XPF and XPG showed the highest negative correlations with drug activity (cisplatin/Et-743 IC_{50}

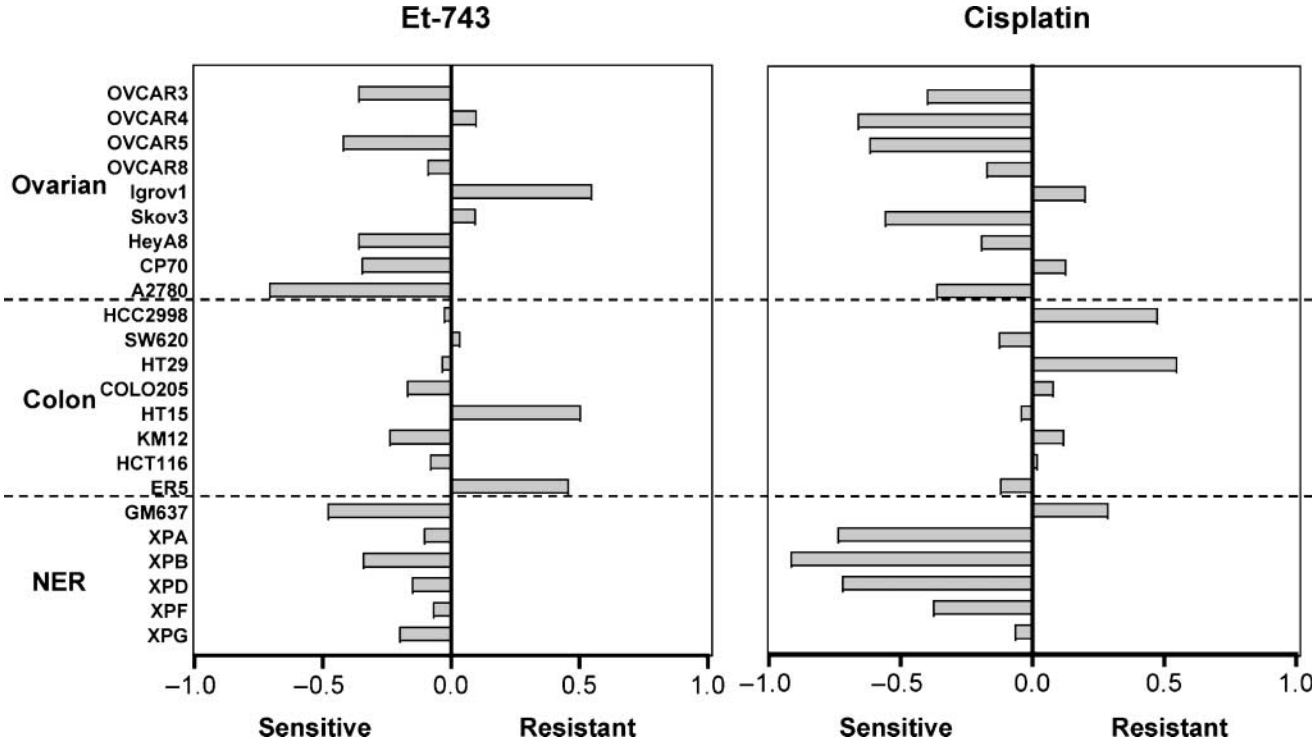

Figure 4. Mean graph drug activity patterns (42) for Et-743 and cisplatin. The sensitivity of Et-743 and cisplatin against tumor cell lines measured using the MTT assay. Indicated values represent the averages of three independent experiments. Values are expressed relative to the mean across all cell lines tested using the equation $-\log_{10}(IC_{50}$ individual cell line - IC_{50} mean). Mean IC_{50} values for all cell lines tested were 5.4×10^{-10} mol/L for Et-743 and 7.4×10^{-6} mol/L for cisplatin.

Table 2. NER biomarkers that predict cisplatin and Et-743 drug activity measured as correlations between mean ''drug preference scores'' and mean NER protein levels for subsets of cell lines

Protein*	All	Ovarian cancer	Colon cancer	XP cell lines
XPA_1	−0.37	0.51	0.10	0.67
XPA_2	−0.26	0.55	0.10	0.64
XPC_1	−0.23	0.36	−0.26	0.85
XPC_2	−0.15	0.14	−0.26	0.85
XPF_1	−0.17	0.56	−0.03	0.93
XPF_2	−0.26	0.62	−0.28	0.90
XPG_1	−0.21	0.15	−0.52	0.88
XPG_2	−0.14	0.39	−0.60	0.91

NOTE: Drug preference score was calculated by subtracting the sensitivity [$-\log_{10}(IC_{50})$] to Et-743 from that to cisplatin. Correlation coefficient, shown in the table, is the correlation between the drug preference score and the XP protein expression levels.

Tissues-of-origin groups: All, all of the groups combined; Ovarian Cancer, ovarian cancer cell lines; Colon Cancer, colon cancer cell lines; XP cell lines, XP-deficient cell lines.

*Nucleotide excision repair proteins (XPA, XPC, XPF, and XPG) profiled across all of tissue-of-origin groups on the reverse-phase protein microarray in duplicates (_1, _2).

difference) across all three tissue-of-origin groups. The increased XPF and XPG protein levels were directly correlated with Et-743 sensitivity and cisplatin resistance, in agreement with our prior studies in NER-deficient isogenic cell pairs (4, 13). However, that result was more effective in predicting drug activity for the XP cell line group than for the ovarian and colon cancer tissue-of-origin groups. All of the TC-NER–deficient patient cell lines (XPA, XPB, XPD, XPF, and XPG) tested are hypersensitive to cisplatin and resistant to Et-743 when compared with their nondeficient counterparts and with normal transformed fibroblasts. That common feature of the XP patient cell lines might explain why XPF and XPG showed higher correlations with drug activity within the XP cell line group than within the ovarian and colon cancer groups.

The ovarian and colon cancer cell lines yielded disparate NER protein expression patterns, making it more difficult to identify a NER biomarker that directly reflects sensitivity [$-\log_{10}(IC_{50})$]. Three of the ovarian lines (OVCAR4, Skov3, and CP70) and four of the colon lines (HCC2998, HT29, HCT15, and ER5) showed opposite sensitivity relationships for Et-743 and cisplatin, as indicated in the graphs of relative mean drug sensitivity. In contrast, the other ovarian and colon cancer cell lines (OVCAR5, OVCAR8, A2780, Igrov1, OVCAR3, HeyA8, SW620, COLO205, KM12, and HCT116) showed the same sensitivity patterns for those drugs, perhaps because of other pathways (e.g., prosurvival, mitogenic, apoptotic, or growth regulatory) involved in drug sensitivity. A microarray gene expression study identified many gene alterations in Igrov1 and the Et-743-resistant Igrov1 ovarian cancer cell line, including upregulation of Rad51, which is important for homologous recombination DNA repair (40). We showed that increased protein expression of Rad51 correlated with Et-743 resistance and cisplatin sensitivity among the ovarian lines. The colon cancer cell lines showed an opposite correlation with Rad51 levels and drug sensitivities, but those correlations would need to be validated in a larger set of cell types.

The Et-743–resistant HCT116 (ER5) colon cancer cell line (13) showed lower Rad51 protein level than did the Et-743–sensitive HCT116 cell line. That finding suggests a possible implication for Rad51 in acquisition of resistance to Et-743 in different cancer types. Other proteins that were increased in the ER5 cell line, p53, MSH2, X-linked inhibitor of apoptosis, and nuclear factor-κB play diverse roles in processes, such as DNA repair, apoptosis, and transcription regulation. Collectively, the data developed here show the difficulty of identifying a single NER biomarker to predict drug sensitivity. The heterogeneity of cancers and the influence of NER-independent pathways probably contribute to this complexity.

Although many factors can influence the cisplatin and Et-743 sensitivity of cell lines, proteomic profiling with the reverse-phase protein microarrays provides a unique opportunity to relate drug sensitivity to key signal transduction proteins. The NER protein profiles presented here will be useful for analyses involving the large library of compounds screened against the NCI-60 and the array of molecular profiles at the DNA, RNA, protein, and small molecule levels available for those cells. We compared the NER protein levels (XPA, XPC, XPF, and XPG) with mRNA levels[7] and found no significant correlation (Pearson correlation coefficient, <0.21). That result is not surprising given that transcript levels may not accurately reflect protein levels. In addition, we compared the NER protein profiles with NCI-60 cell line compound sensitivities and found a negative correlation between sensitivity to alkylating agents (nitrosoureas) and XPA protein levels in the ovarian and colon cancer cell lines. Those findings are consistent with the value of XPA as a protein biomarker for NER. The NER protein profiles presented here will be useful for future analyses involving the large library of compounds screened against the NCI-60 and the array of molecular profiles at the DNA, RNA, protein, and small molecule levels available for those cells.

It is clear that cell lines are not fully representative of tumors from patients, but they do have the advantages of reproducibility, availability, and homogeneity in cell lineage. We previously used colon and ovarian lines as the starting point for identification of molecular markers for differential diagnosis between advanced colon and ovarian cancers (41). That study suggested that useful information from patients' tumors is retained in cultured cells. Further studies in tumors to correlate the NER protein levels with clinical data will clarify the biochemical roles of the NER proteins and their potential as therapeutic markers. Such a study might entail laser capture microdissection of tumor cells from biopsy materials and application of the resulting samples to reverse-phase protein arrays for mapping of protein pathways implicated in

[7] Derived from http://discover.nci.nih.gov/cellminer.

drug response. In summary, the work reported here on quantitation of the NER proteins in cancer cell lines may provide the basis for such future studies, with the goal of developing more effective molecularly targeted, patient-tailored therapies.

Acknowledgments

We thank Kurt W. Kohn, Bill Bonner, Mirit Aladjem, Rick Wood, Beate Koberle, John Bradsher, Larry Hayward, Gregory Aune, and Olivier Sordet for useful discussions; Glenda Kohlhagen for preliminary experiments; Sylvia Major for use of AbMiner; and Jareer Kassis for reviewing a draft of the manuscript.

References

1. Kelland L. The resurgence of platinum-based cancer chemotherapy. Nat Rev Cancer 2007;7:573 – 84.

2. McGuire WP, Ozols RF. Chemotherapy of advanced ovarian cancer. Semin Oncol 1998;25:340 – 8.

3. Reed E. ERCC1 and clinical resistance to platinum-based therapy. Clin Cancer Res 2005;11:6100 – 2.

4. Furuta T, Ueda T, Aune G, Sarasin A, Kraemer KH, Pommier Y. Transcription-coupled nucleotide excision repair as a determinant of cisplatin sensitivity of human cells. Cancer Res 2002;62:4899 – 902.

5. Arnould S, Hennebelle I, Canal P, Bugat R, Guichard S. Cellular determinants of oxaliplatin sensitivity in colon cancer cell lines. Eur J Cancer 2003;39:112 – 9.

6. Hoeijmakers JH. Genome maintenance mechanisms for preventing cancer. Nature 2001;411:366 – 74.

7. Takebayashi Y, Nakayama K, Kanzaki A, et al. Loss of heterozygosity of nucleotide excision repair factors in sporadic ovarian, colon and lung carcinomas: implication for their roles of carcinogenesis in human solid tumors. Cancer Lett 2001;174:115 – 25.

8. Koberle B, Masters JR, Hartley JA, Wood RD. Defective repair of cisplatin-induced DNA damage caused by reduced XPA protein in testicular germ cell tumours. Curr Biol 1999;9:273 – 6.

9. Verweij J. Ecteinascidin-743 (ET-743): early test or effective treatment in soft tissue sarcomas? J Clin Oncol 2005;23:5420 – 3.

10. Fayette J, Coquard IR, Alberti L, et al. ET-743: a novel agent with activity in soft-tissue sarcomas. Curr Opin Oncol 2006;18:347 – 53.

11. Pommier Y, Kohlhagen G, Bailly C, Waring M, Mazumder A, Kohn KW. DNA sequence- and structure-selective alkylation of guanine N2 in the DNA minor groove by ecteinascidin 743, a potent antitumor compound from the Caribbean tunicate *Ecteinascidia turbinata*. Biochemistry 1996; 35:13303 – 9.

12. Zewail-Foote M, Hurley LH. Ecteinascidin 743: a minor groove alkylator that bends DNA toward the major groove. J Med Chem 1999; 42:2493 – 7.

13. Takebayashi Y, Pourquier P, Zimonjic DB, et al. Antiproliferative activity of ecteinascidin 743 is dependent upon transcription-coupled nucleotide-excision repair. Nat Med 2001;7:961 – 6.

14. Erba E, Bergamaschi D, Bassano L, et al. Ecteinascidin-743 (ET-743), a natural marine compound, with a unique mechanism of action. Eur J Cancer 2001;37:97 – 105.

15. Nishizuka S, Charboneau L, Young L, et al. Proteomic profiling of the NCI-60 cancer cell lines using new high-density reverse-phase lysate microarrays. Proc Natl Acad Sci U S A 2003;100:14229 – 34.

16. Shankavaram UT, Reinhold WC, Nishizuka S, et al. Transcript and protein expression profiles of the NCI-60 cancer cell panel: an integromic microarray study. Mol Cancer Ther 2007;6:820 – 32.

17. Paweletz CP, Charboneau L, Bichsel VE, et al. Reverse phase protein microarrays which capture disease progression show activation of pro-survival pathways at the cancer invasion front. Oncogene 2001;20: 1981 – 9.

18. Shoemaker RH. The NCI60 human tumour cell line anticancer drug screen. Nat Rev Cancer 2006;6:813 – 23.

19. Weinstein JN. Spotlight on molecular profiling: ''integromic'' analysis of the NCI-60 cancer cell lines. Mol Cancer Ther 2006;5:2601 – 5.

20. Weinstein JN, Myers TG, O'Connor PM, et al. An information-intensive approach to the molecular pharmacology of cancer. Science 1997;275:343 – 9.

21. Scherf U, Ross DT, Waltham M, et al. A gene expression database for the molecular pharmacology of cancer. Nat Genet 2000;24: 236 – 44.

22. Rochette PJ, Bastien N, McKay BC, Therrien JP, Drobetsky EA, Drouin R. Human cells bearing homozygous mutations in the DNA mismatch repair genes hMLH1 or hMSH2 are fully proficient in transcription-coupled nucleotide excision repair. Oncogene 2002;21:5743 – 52.

23. Umar A, Koi M, Risinger JI, et al. Correction of hypermutability, *N*-methyl-*N*′-nitro-*N*-nitrosoguanidine resistance, and defective DNA mismatch repair by introducing chromosome 2 into human tumor cells with mutations in MSH2 and MSH6. Cancer Res 1997;57:3949 – 55.

24. Oshima RG, Baribault H, Caulin C. Oncogenic regulation and function of keratins 8 and 18. Cancer Metastasis Rev 1996;15:445 – 71.

25. McCluggage WG, Wilkinson N. Metastatic neoplasms involving the ovary: a review with an emphasis on morphological and immunohistochemical features. Histopathology 2005;47:231 – 47.

26. Washio F, Ueda M, Ito A, Ichihashi M. Higher susceptibility to apoptosis following ultraviolet B irradiation of xeroderma pigmentosum fibroblasts is accompanied by upregulation of p53 and downregulation of bcl-2. Br J Dermatol 1999;140:1031 – 7.

27. D'Incalci M, Jimeno J. Preclinical and clinical results with the natural marine product ET-743. Expert Opin Investig Drugs 2003;12:1843 – 53.

28. Grasselli G, Malossi A, Colombo N, et a. Phase I and pharmacokinetic (PK) study of ecteinascidin-743 (ET, trabectedin) and cisplatin (P) combination in pre-treated patients (pts) with selected advanced solid tumors. Proc Am Soc Clin Oncol 2003;22:542.

29. Parma G, Bauer J, Noberasco C, et al. Yondelis TM (Et-743, trabectedin) antitumor activity in ovarian cancer patients prestreated with platinum-taxane regimens. Ann Oncol 2003;14:iii52.

30. Sabbatini P. New agents and new formulations for the treatment of ovarian cancer. Clin Adv Hematol Oncol 2005;3:840 – 2.

31. Sessa C, De Braud F, Perotti A, et al. Trabectedin for women with ovarian carcinoma after treatment with platinum and taxanes fails. J Clin Oncol 2005;23:1867 – 74.

32. Ganesan AK, Hunt J, Hanawalt PC. Expression and nucleotide excision repair of a UV-irradiated reporter gene in unirradiated human cells. Mutat Res 1999;433:117 – 26.

33. Welsh C, Day R, McGurk C, Masters JR, Wood RD, Koberle B. Reduced levels of XPA, ERCC1 and XPF DNA repair proteins in testis tumor cell lines. Int J Cancer 2004;110:352 – 61.

34. Koberle B, Grimaldi KA, Sunters A, Hartley JA, Kelland LR, Masters JR. DNA repair capacity and cisplatin sensitivity of human testis tumour cells. Int J Cancer 1997;70:551 – 5.

35. Ferry KV, Hamilton TC, Johnson SW. Increased nucleotide excision repair in cisplatin-resistant ovarian cancer cells: role of ERCC1-XPF. Biochem Pharmacol 2000;60:1305 – 13.

36. Yu JJ, Mu C, Dabholkar M, Guo Y, Bostick-Bruton F, Reed E. Alternative splicing of ERCC1 and cisplatin-DNA adduct repair in human tumor cell lines. Int J Mol Med 1998;1:617 – 20.

37. Britten RA, Liu D, Tessier A, Hutchison MJ, Murray D. ERCC1 expression as a molecular marker of cisplatin resistance in human cervical tumor cells. Int J Cancer 2000;89:453 – 7.

38. Stevens EV, Posadas EM, Davidson B, Kohn EC. Proteomics in cancer. Ann Oncol 2004;15 Suppl 4:iv167 – 71.

39. Stevens EV, Liotta LA, Kohn EC. Proteomic analysis for early detection of ovarian cancer: a realistic approach? Int J Gynecol Cancer 2003;13 Suppl 2:133 – 9.

40. Marchini S, Marrazzo E, Bonomi R, et al. Molecular characterisation of two human cancer cell lines selected *in vitro* for their chemotherapeutic drug resistance to ET-743. Eur J Cancer 2005;41:323 – 33.

41. Nishizuka S, Chen ST, Gwadry FG, et al. Diagnostic markers that distinguish colon and ovarian adenocarcinomas: identification by genomic, proteomic, and tissue array profiling. Cancer Res 2003;63:5243 – 50.

42. Paull KD, Shoemaker RH, Hodes L, et al. Display and analysis of patterns of differential activity of drugs against human tumor cell lines: development of mean graph and COMPARE algorithm. J Natl Cancer Inst 1989;81:1088 – 92.